JOURNAL OF COMPUTATIONAL PHYSICS **126,** 449–467 (1996)
ARTICLE NO. 0149

Numerical Schemes for Hyperbolic Conservation Laws with Stiff Relaxation Terms

SHI JIN*,[1] AND C. DAVID LEVERMORE†,[2]

*School of Mathematics, Georgia Institute of Technology, Atlanta, Georgia 30332; †Department of Mathematics, University of Arizona, Tucson, Arizona 85721

Received February 22, 1995; revised February 20, 1996

Hyperbolic systems often have relaxation terms that give them a partially conservative form and that lead to a long-time behavior governed by reduced systems that are parabolic in nature. In this article it is shown by asymptotic analysis and numerical examples that semidiscrete high resolution methods for hyperbolic conservation laws fail to capture this asymptotic behavior unless the small relaxation rate is resolved by a fine spatial grid. We introduce a modification of higher order Godunov methods that possesses the correct asymptotic behavior, allowing the use of coarse grids (large cell Peclet numbers). The idea is to build into the numerical scheme the asymptotic balances that lead to this behavior. Numerical experiments on 2×2 systems verify our analysis.

1. INTRODUCTION

Hyperbolic systems of partial differential equations that arise in applications often have relaxation terms that give the system a partially conservative form and lead to a long-time behavior governed by a reduced system that is parabolic in nature. Such systems are found in relaxing gas theory [8, 46], multiphase flow [15], and turbulence modeling [13, 30], where the relaxation terms describe thermal coupling, phase coupling or turbulent kinematics, respectively. They also arise in kinetic theory [2, 5, 33, 34], where the relaxation terms model the interaction of particles.

One of the simplest such systems is the p-system with damping:

$$\begin{aligned} \partial_t h + \partial_x w &= 0, \\ \partial_t w + \partial_x p(h) &= -(1/\tau) w. \end{aligned} \tag{1.1}$$

Here the parameter $\tau > 0$ is the relaxation time for the system, which is hyperbolic provided $p'(h) > 0$. The system can be viewed as the isentropic Euler equations in Lagrangian form with a drag term in the momentum equation. It was studied by Hsiao and Liu [22] who showed that its solutions exhibit a long-time behavior governed by

$$\partial_t h - \tau \partial_{xx} p(h) = 0, \qquad w = -\tau \partial_x p(h). \tag{1.2}$$

The first equation above is sometimes referred to as the porous media equation, in which context the second plays the role of Darcy's law.

A somewhat more general system with relaxation that we will use to illustrate the subsequent theory is

$$\begin{aligned} \partial_t h + \partial_x w &= 0, \\ \partial_t w + \partial_x p(h) &= -(1/\tau)(w - f(h)), \end{aligned} \tag{1.3}$$

where $\tau > 0$ is again the relaxation time. We shall assume $p'(h) > 0$, whereby the system (1.3) is hyperbolic with characteristic velocities of $\pm\sqrt{p'(h)}$. The long-time behavior of its solutions are governed by

$$\partial_t h + \partial_x f(h) = \tau \partial_x [(p'(h) - f'(h)^2) \partial_x h], \tag{1.4a}$$

$$w = f(h) - \tau (p'(h) - f'(h)^2) \partial_x h, \tag{1.4b}$$

provided that the characteristic velocity $f'(h)$ associated with (1.4a) when $\tau = 0$ interlaces with those of system (1.3) as

$$-\sqrt{p'(h)} < f'(h) < \sqrt{p'(h)}. \tag{1.5}$$

This stability condition is a general feature of such approximations. It can be understood from several points of view. First, from a phenomenological viewpoint, this ordering of the velocities is consistent with causality when $\tau = 0$ in (1.4a). Second, for $\tau > 0$ this condition reflects the requirement that the diffusion coefficient in (1.4a) be nonnegative. Finally, and most fundamentally, a spatially homogeneous equilibrium of the system (1.3) in the form $(h, w) = (\bar{h}, f(\bar{h}))$ for any constant $\bar{h}$ is stable if and only if $h = \bar{h}$ satisfies (1.5) (see [48]). Indeed, if (1.5) is not

[1] E-mail address: jin@math.gatech.edu.
[2] E-mail address: lvrmr@math.arizona.edu.

0021-9991/96 $18.00

satisfied then a simple linear analysis shows that some perturbations can grow at rates on the order of $1/\tau$.

The relation between solutions of system (1.3) and those of Eq. (1.4) was studied in [6, 7, 36]. A critical nondimensional parameter ε is the ratio of the distance a typical sound wave travels (at speed $c = \sqrt{p'(h)}$) over the relaxation time τ to a typical gradient length L:

$$\varepsilon = c\tau/L. \tag{1.6}$$

When $\varepsilon \ll 1$, the relaxation term is called *stiff*. In this regime the solutions of the original system (1.3) can be studied by a formal asymptotic expansion in ε which is analogous to the Chapman–Enskog expansion of kinetic theory [7]. It is found that their behavior is governed by the parabolic approximation (1.4), whereby ε measures the validity of the parabolic approximation.

This formal relationship was justified in [7]. There system (1.3) was considered for a fixed $p(h)$ as τ, and thereby ε defined by (1.6), becomes smaller. It was rigorously proved that if $(h_\varepsilon, w_\varepsilon)$ is a family of solutions of (1.3) with fixed initial data then as ε tends to zero the functions h_ε converge to h, the viscosity solution of

$$\partial_t h + \partial_x f(h) = 0, \tag{1.7}$$

with the same initial data. A weakly nonlinear limit was also established to solutions of a Burgers equation derived from (1.4a). More specifically, given any constant $\bar{h}$ such that $f'(\bar{h}) \neq 0$, a family of solutions $(h_\varepsilon, w_\varepsilon)$ of (1.3) was considered in the form

$$\begin{aligned} h_\varepsilon(x,t) &= \bar{h} + \varepsilon \tilde{h}_\varepsilon(\varepsilon t, x - f'(\bar{h})t), \\ w_\varepsilon(x,t) &= f(\bar{h}) + \varepsilon\, \tilde{w}_\varepsilon(\varepsilon t, x - f'(\bar{h})t), \end{aligned} \tag{1.8}$$

with the initial data for $(\tilde{h}_\varepsilon, \tilde{w}_\varepsilon)$ independent of ε. Then, as ε tends to zero, the functions $\tilde{h}_\varepsilon = \tilde{h}_\varepsilon(s, y)$ were shown to converge to $\tilde{h} = \tilde{h}(s, y)$, the solution of the Burgers equation

$$\partial_s \tilde{h} + f''(\bar{h})\tilde{h}\partial_y \tilde{h} = (p'(\bar{h}) - f'(\bar{h})^2)\partial_{yy}\tilde{h}, \tag{1.9}$$

with the same initial data. The relationship between the rigorous limit and the claimed long-time behavior of solutions of (1.3) is seen from the fact that (1.9) is the formal long-time/weakly nonlinear approximation of (1.4a) that is consistent with the scalings in (1.8). Analogs of these results were established in [7] for the general class of 2×2 systems that we will treat in Section 4.

In general an $N \times N$ hyperbolic system of conservation laws with relaxation terms has the form

$$\partial_t u + \partial_x F(u) = q(u). \tag{1.10}$$

We assume that the relaxation term $q(u)$ determines uniquely the stable local equilibria $u = \mathscr{E}(v)$ for n $(n < N)$ independent conserved quantities v. Consider all eigenvalues of $\partial_u q$. We define τ, the relaxation time, as the reciprocal of the largest eigenvalue in absolute value when evaluated at the local equilibria $u = \mathscr{E}(v)$. The eigenvalue corresponding to a local equilibrium is nonnegative when evaluated at a local equilibrium. Let c be the absolute value of the largest characteristic speed of the system, or the largest characteristic speed evaluated at the local equilibria (our numerical experiments show little difference between these two choices). One can then define the nondimensional relaxation parameter ε as in (1.6). This system becomes stiff if $\varepsilon \ll 1$. In such a regime the behavior of the locally conserved quantity v is asymptotically governed by a system of convection–diffusion equations, analogous to (1.4a). There have been many theoretical investigations of such systems in this regime (e.g., [6, 7, 34, 35]). In particular, the general framework of the parabolic approximation for $N \times N$ systems in any spatial dimension was laid down in [7].

In this article we are concerned with the numerical methods for hyperbolic systems with stiff relaxation terms. We will only study semidiscrete numerical schemes, leaving the time variable continuous. This is not because we advocate a "method of lines" approach to these problems; we do not. But rather because that what we present will be more of a procedure than a prescription, and this simpler setting allows us to expose the basic ideas more clearly. Of course, as one lets the time step approach zero in a fully discrete scheme it becomes semidiscrete; the results presented below apply to the limiting scheme. In this way our analysis will provide constraints for every numerical scheme.

We will consider a uniform spatial grid with nodes $x_{j+1/2}$ and a cell width $\Delta x = x_{j+1/2} - x_{j-1/2}$. The uniformity of the grid is not essential to our analysis but does serve to simplify our presentation. Given any function u, we denote its nodal values by $u_{j+1/2} = u(x_{j+1/2})$ and its cell-average values by

$$u_j = \frac{1}{\Delta x}\int_{x_{j-1/2}}^{x_{j+1/2}} u\, dx. \tag{1.11}$$

By averaging the conservation law (1.10) over the jth cell one obtains

$$\partial_t u_j + \frac{F(u_{j+1/2}) - F(u_{j-1/2})}{\Delta x} = q_j, \tag{1.12}$$

where the cell-average source is defined by

$$q_j = \frac{1}{\Delta x}\int_{x_{j-1/2}}^{x_{j+1/2}} q(u)\, dx.$$

Now let U denote a numerical approximation to the cell-averaged values of u; we suppose that U satisfies a spatial discretization of (1.10) in the conservative form

$$\partial_t U_j + \frac{F_{j+1/2} - F_{j-1/2}}{\Delta x} = Q_j. \tag{1.13}$$

A discretization is then specified by relating the nodal flux values $F_{j+1/2}$ and the cell-average source Q_j to the cell-averaged values U_j in accordance with (1.12) and (1.13).

The central issue in numerical simulation of a stiff relaxation system is how well the discretization resolves the small relaxation scale. The spatial resolution of a given solution of a scheme is measured by the smallness of the nondimensional parameter

$$\delta = \Delta x / L. \tag{1.14}$$

We will show that, in order to study the long-time accuracy of a scheme like (1.13), it is natural to introduce a second nondimensional parameter, namely, the cell Peclet number (or cell Reynolds number). The cell Peclet number Pe measures the spatial resolution of the relaxation scale and is defined as

$$\mathrm{Pe} \equiv \frac{\delta}{\varepsilon} = \frac{\Delta x}{c\tau}. \tag{1.15}$$

A grid will be called coarse (relative to the relaxation scale) when $\mathrm{Pe} \gg 1$, fine if $\mathrm{Pe} \ll 1$, and intermediate otherwise.

The development of numerical schemes to solve hyperbolic systems with source terms has been an active area of research in the past two decades (e.g., [14, 35, 38–41, 45]), most of which have considered the importance of the steady state balance in devising numerical solutions. To our knowledge there has been no work that uses the asymptotics that lead from the original system to the reduced parabolic system, either as a guide in deriving a numerical method, or as a tool in analyzing the behavior of these numerical methods. Of course, such an approach is restricted to systems that possess such or similar asymptotic regimes. Other early literature studied stiff source problems in reactive flows, where an incorrect numerical shock speed was found when the reaction time scale ε was not resolved numerically [1, 9, 11, 12, 18, 32]. These works focused on source terms that take on a more complicated form than those considered in this article (for example, exhibiting multiple equilibria, or the characteristic speeds of the original system and the local equilibrium system do not interlace), and the resulting long-time behavior can be quite different. Also related to our work are those of Harabetian's [19, 20], in which the dissipative effects of numerical schemes for viscous hyperbolic systems have been studied without specifically addressing the issue of stiff relaxation.

In the absence of lower order relaxation terms, these systems are just systems of conservation laws and one could employ a higher order Godunov [44, 10, 31, 21] type scheme to evaluate the fluxes. These schemes properly capture the discontinuous features of the solutions. However, when the relaxation becomes stiff, it is computationally impractical to spatially, as well as temporally, resolve the small relaxation scale. Therefore, it is desirous to ensure that the scheme properly captures the parabolic behavior even when $\mathrm{Pe} \gg 1$. An example of such numerical schemes arises in linear transport theory, where the density of particles undergoing collisions with a background medium will solve the diffusion equation in the limit of vanishing mean free path [28, 29]. In this case much progress has been made in developing schemes that incorporate boundary layers and material interfaces [17, 25, 26]. However, little attention has been given to this problem for the case of genuinely nonlinear systems; in such cases the difficulties of properly capturing the development and evolution of discontinuities complicates the picture.

Our first objective in this article is to show through asymptotic analysis and numerical experiments that, in the presence of stiff relaxation terms, most shock-capturing schemes fail to capture the proper parabolic behavior when $\mathrm{Pe} \gg 1$. Indeed, by considering only semidiscrete schemes we will show that this difficulty is one of spatial, as well as temporal, resolution.

Our second objective in this article is to develop semidiscrete numerical schemes for such systems that are modern high-order shock-capturing schemes, yet that will handle correctly the difficulties involving lower order relaxation terms. A good discretization meeting this criterion would allow the use of a coarse grid to resolve spatial features and ultimately allow the implementation of an implicit temporal scheme to enable one to economically compute the longer time scales of interest. We show that such spatial discretizations can be realized by properly modifying their numerical fluxes. The main idea we utilize is to simply build the proper asymptotic balances into the spatial difference scheme. We began such an investigation in [23]. In particular, in a spirit close to the idea of modeling the flow as piecewise steady [14, 40, 45], a semidiscrete numerical scheme will be said to have the correct parabolic behavior if the asymptotics that lead from the hyperbolic system to the parabolic approximation in continuous space are mimicked in discrete space. That is to say, as $\mathrm{Pe} \to \infty$, the numerical scheme will behave asymptotically as a good discretization of the parabolic system.

In Section 2 we analyze the linear telegraph equations to show that higher order Godunov schemes are usually too dissipative to capture the correct parabolic behavior when $\mathrm{Pe} \gg 1$. More specifically, we show that in this regime,

these schemes introduce numerical dissipation that overwhelms the physical dissipation. We compare such a behavior to the behavior of those schemes that do take into account the stiff source term in the approximation. These include the piecewise steady approximation and a modified upwind scheme, and we will show that they capture the proper parabolic behavior even when Pe $\gg 1$.

In Section 3 we examine the general 2×2 p-system (1.3), where the long-term behavior is governed by a convection–diffusion equation. Here the presence of convection in the long-time approximation complicates the picture, and upwind schemes may become excessively diffusive when Pe $\gg 1$. We will introduce a new numerical flux based on higher order Godunov methods that achieve two goals. First, it eliminates the excessive numerical dissipation that arises in these schemes when Pe $\gg 1$. Second, solutions of the resulting scheme possess a long-time behavior that is governed by Godunov schemes of the same order for the correct parabolic equation (1.4) when Pe $\gg 1$. In regimes where the long-time hyperbolic behavior is important, such schemes capture the nearly discontinuous phenomena associated with the corresponding nonlinear convection term. In regimes where the parabolic behavior becomes significant, these schemes also capture the dissipative nature. Numerical experiments show that these schemes achieve good results on coarse grids.

In Section 4 we show how the same ideas can be applied when treating more general 2×2 systems. These schemes are then illustrated with numerical experiments using the idealized river equations. Finally, in Section 5 we make some concluding remarks where, among other things, we address the relevance of this work to temporally discrete schemes. While our analysis and numerical experiments will be performed on 2×2 systems, it is straightforward to extend our results to $N \times N$ systems of the form (1.10).

2. DISSIPATION: A LINEAR MODEL

2.1. *The Model*

In this section we consider an illustrative nondimensional linear model. When $p(h) = h$ and $\tau = \varepsilon$ in system (1.1), it becomes

$$\begin{aligned} &\partial_t h + \partial_x w = 0, \\ &\partial_t w + \partial_x h = -(1/\varepsilon) w, \end{aligned} \tag{2.1}$$

which are also known as the telegraph equations [27]. This system has characteristic speeds ± 1. Accordingly, its solutions exhibit an approximate parabolic behavior (1.2) governed by

$$\partial_t h - \varepsilon \partial_{xx} h = 0, \quad w = -\varepsilon \partial_x h. \tag{2.2}$$

Here h approximately satisfies a linear heat equation.

This behavior can also be illustrated explicitly using Fourier modes. Note that

$$h(t, x) = \hat{h} e^{-\lambda t + i\xi x}, \quad w(t, x) = \hat{w} e^{-\lambda t + i\xi x}$$

will solve (2.1) for a nondimensional wavenumber ξ, provided λ satisfies

$$\lambda = \lambda_{\pm} \equiv \frac{1}{2\varepsilon} \pm \frac{1}{2\varepsilon} \sqrt{1 - 4\varepsilon^2 \xi^2},$$

and $i\xi \hat{w}_{\pm} = \lambda_{\pm} \hat{h}_{\pm}$. As ε tends to zero, while holding ξ fixed, these relations become

$$\begin{aligned} &\lambda_+ = 1/\varepsilon + O(\varepsilon), \quad && \hat{h}_+ = -i\varepsilon\xi \hat{w}_+ + O(\varepsilon^3); \\ &\lambda_- = \varepsilon \xi^2 + O(\varepsilon^3), \quad && \hat{w}_- = -i\varepsilon\xi \hat{h}_- + O(\varepsilon^3). \end{aligned} \tag{2.3}$$

One can see that the λ_+ mode decays rapidly to zero as t increases while the λ_- mode corresponds to the parabolic behavior described by (2.2).

The discretization (1.13) applied to the telegraph equations (2.1) yields

$$\begin{aligned} &\partial_t H_j + \frac{W_{j+1/2} - W_{j-1/2}}{\delta} = 0, \\ &\partial_t W_j + \frac{H_{j+1/2} - H_{j-1/2}}{\delta} = -\frac{1}{\varepsilon} W_j, \end{aligned} \tag{2.4}$$

where δ is the nondimensional grid size defined in (1.14). In the next five subsections, the numerical fluxes $H_{j+1/2}$ and $W_{j+1/2}$ will be determined in terms of H_j and W_j by five different upwind difference schemes.

2.2. *The Upwind Scheme*

By adding and subtracting the two equations in (2.1), one easily finds the diagonalized system

$$\begin{aligned} &\partial_t (w + h) + \partial_x (w + h) = -(1/\varepsilon) w, \\ &\partial_t (w - h) - \partial_x (w - h) = (1/\varepsilon) w. \end{aligned} \tag{2.5}$$

The quantities $w \pm h$ move with velocities ± 1, respectively, and locally relax toward their average value. They would be the Riemann invariants of system (2.1) in the absence of the relaxation term ($\varepsilon = \infty$).

To determine the nodal values $H_{j+1/2}$ and $W_{j+1/2}$, the so-called upwind scheme assumes that the solution is piecewise constant and then selects the values of $w \pm h$ from the direction "upwind" of their respective characteristic velocities. Specifically, it selects

$$(W+H)_{j+1/2} = (W+H)_j,$$
$$(W-H)_{j+1/2} = (W-H)_{j+1}, \tag{2.6}$$

which gives the nodal values

$$H_{j+1/2} = \frac{H_j + H_{j+1}}{2} - \frac{W_{j+1} - W_j}{2},$$
$$W_{j+1/2} = -\frac{H_{j+1} - H_j}{2} + \frac{W_j + W_{j+1}}{2}. \tag{2.7}$$

The values of $H_{j-1/2}$ and $W_{j-1/2}$ are obtained simply by translating j to $j-1$ in (2.7). The use of (2.7) in the discrete equation (2.4) results in the scheme

$$\partial_t H_j - \frac{H_{j+1} - 2H_j + H_{j-1}}{2\delta} + \frac{W_{j+1} - W_{j-1}}{2\delta} = 0,$$
$$\partial_t W_j - \frac{W_{j+1} - 2W_j + W_{j-1}}{2\delta} + \frac{H_{j+1} - H_{j-1}}{2\delta} = -\frac{1}{\varepsilon} W_j. \tag{2.8}$$

The modified equations [47] corresponding to this scheme are

$$\partial_t h + \partial_x w = \frac{\delta}{2}\partial_{xx} h - \frac{\delta^2}{6}\partial_{xxx} w,$$
$$\partial_t w + \partial_x h = -\frac{1}{\varepsilon} w + \frac{\delta}{2}\partial_{xx} w - \frac{\delta^2}{6}\partial_{xxx} h.$$

These show the first-order nature of the upwind scheme (2.8) for fixed ε.

The "parabolic" behavior of this scheme is obtained in the same fashion as going from (2.1) to (2.2), by a formal asymptotic expansion for small ε (while holding δ fixed). The second equation of (2.8) gives

$$W_j = -\varepsilon \frac{H_{j+1} - H_{j-1}}{2\delta} + O(\varepsilon^2).$$

After substituting this into the first equation of (2.8) and dropping the $O(\varepsilon^2)$ terms one obtains

$$\partial_t H_j - \frac{H_{j+1} - 2H_j + H_{j-1}}{2\delta} - \varepsilon \frac{H_{j+2} - 2H_j + H_{j-2}}{(2\delta)^2} = 0. \tag{2.9}$$

A Fourier analysis of the upwind scheme (2.8) shows that only long wavelength modes will survive to be governed by (2.9). Hence, the whole story of the long-time behavior will be told by the modified equation corresponding to (2.9), which is

$$\partial_t h - \varepsilon \partial_{xx} h = \frac{\delta}{2}\partial_{xx} h. \tag{2.10}$$

In order to have the correct long-time behavior, it is essential that Eq. (2.10) be an accurate approximation of the first equation in (2.2). This will be the case only if $\mathrm{Pe} = \delta/\varepsilon \ll 1$; i.e., the grid is fine. However, if either $\mathrm{Pe} \sim 1$ or $\mathrm{Pe} \gg 1$ then the numerical dissipation rate of order δ will either be comparable or dominate the physical dissipation of order ε. In either case, the numerical solution will dissipate faster than the physical one, dissipating even faster as the grid coarsens. Thus, for intermediate or coarse grids the upwind scheme will not give the correct parabolic behavior for this problem.

2.3. *The van Leer Scheme*

In order to derive a higher order numerical scheme, van Leer [44] used piecewise linear functions to interpolate the values of the cell-edge $U_{j+1/2}$ from the cell-center U_j. For the scalar linear advection equation,

$$\partial_t u + a\partial_x u = 0,$$

the scheme is as follows. Suppose that each U_j is interpreted as the cell-averaged value of u over the jth cell. Approximate u by a piecewise linear function that over x in the jth cell $[x_{j-1/2}, x_{j+1/2}]$ takes the form

$$U_j(x) = U_j + m_j(x - x_j), \tag{2.11}$$

where $x_j = \frac{1}{2}(x_{j-1/2} + x_{j+1/2})$ is the midpoint of the cell, so that the average of $U_j(x)$ over the jth cell is U_j. If the unknown m_j is chosen by requiring that the average of $U_j(x)$ over either the $(j-1)$th or the $(j+1)$th cell to be U_{j-1} or U_{j+1}, respectively, then in the former case it takes the value

$$m_{j-1/2} = \frac{U_j - U_{j-1}}{\delta},$$

while in the latter case it takes the value

$$m_{j+1/2} = \frac{U_{j+1} - U_j}{\delta}.$$

For uniform grids a natural candidate for m_j is

$$\overline{m}_j = \frac{m_{j-1/2} + m_{j+1/2}}{2} = \frac{U_{j+1} - U_{j-1}}{2\delta}, \tag{2.12}$$

which is a second-order approximation to the slope of u at x_j. In order to preserve the monotonicity of the solution we choose the numerical slope m_j by the so-called flux-limited modification of $\overline{m}_j$ as

$$m_j = \begin{cases} 0, & \text{if } m_{j-1/2} m_{j+1/2} \le 0, \\ \overline{m}_j \min\left\{ 2\dfrac{m_{j-1/2}}{\overline{m}_j}, 2\dfrac{m_{j+1/2}}{\overline{m}_j}, 1 \right\}, & \text{otherwise.} \end{cases} \quad (2.13)$$

One then defines the nodal values to be the upwind value of this piecewise linear interpolant, which are given by

$$U_{j+1/2} = \begin{cases} U_j(x_{j+1/2}), & \text{if } a > 0; \\ U_{j+1}(x_{j+1/2}), & \text{if } a < 0. \end{cases} \quad (2.14)$$

For nonlinear scalar equations one generalizes (2.14) by setting $U_{j+1/2}$ equal to the value along $x = x_{j+1/2}$ of the solution of the Riemann problem with left and right data given by $U_j(x_{j+1/2})$ and $U_{j+1}(x_{j+1/2})$, respectively. This method extends to systems by the local field-by-field characteristic decomposition.

For the telegraph equations (2.1) the above procedure is applied to each component of the diagonalized system (2.5) to obtain

$$\begin{aligned} (W + H)_{j+1/2} &= W_j + H_j + m_j^+ (x_{j+1/2} - x_j), \\ (W - H)_{j+1/2} &= W_{j+1} - H_{j+1} + m_{j+1}^- (x_{j+1/2} - x_{j+1}), \end{aligned} \quad (2.15)$$

where $m_j^\pm$ is the slope given by (2.13) corresponding to the quantities $W \pm H$. If the solution is resolved by the grid then away from local extrema of $w \pm h$ the flux-limiters do not take effect and the slope takes the value $\overline{m}_j$ of (2.12) corresponding to $W \pm H$. Consequently, solving (2.15) for the nodal quantities and substituting the result into the discrete equation (2.4) leads to

$$\partial_t H_j + \frac{H_{j+2} - 4H_{j+1} + 6H_j - 4H_{j-1} + H_{j-2}}{8\delta} + \frac{-W_{j+2} + 6W_{j+1} - 6W_{j-1} + W_{j-2}}{8\delta} = 0, \quad (2.16a)$$

$$\partial_t W_j + \frac{-H_{j+2} + 6H_{j+1} - 6H_{j-1} + H_{j-2}}{8\delta} + \frac{W_{j+2} - 4W_{j+1} + 6W_j - 4W_{j-1} + W_{j-2}}{8\delta} = -\frac{1}{\varepsilon} W_j. \quad (2.16b)$$

The modified equations corresponding to (2.16) are

$$\begin{aligned} \partial_t h + \partial_x w &= \frac{\delta^2}{2} \partial_{xxx} w - \frac{\delta^3}{8} \partial_{xxxx} h, \\ \partial_t w + \partial_x h &= -\frac{1}{\varepsilon} w + \frac{\delta^2}{2} \partial_{xxx} h - \frac{\delta^3}{8} \partial_{xxxx} w. \end{aligned} \quad (2.17)$$

This shows the second-order accuracy of the van Leer scheme away from local extrema of $w \pm h$ for the telegraph equations (2.1) while holding ε fixed.

The behavior of this scheme for small ε while holding δ fixed is as follows. By assuming only long wavelengths survive and again avoiding local extrema, the flux-limiting (2.13) can be neglected and (2.16b) gives

$$W_j = -\varepsilon \frac{-H_{j+2} + 6H_{j+1} - 6H_{j-1} + H_{j-2}}{8\delta} + O(\varepsilon^2).$$

After substituting this into (2.16a) and dropping the $O(\varepsilon^2)$ terms, one finds

$$\begin{aligned} \partial_t H_j + \frac{H_{j+2} - 4H_{j+1} + 6H_j - 4H_{j-1} + H_{j-2}}{8\delta} \\ - \varepsilon \frac{1}{(8\delta)^2} [H_{j+4} - 12H_{j+3} + 36H_{j+2} \\ + 12H_{j+1} - 74H_j + 12H_{j-1} + 36H_{j-2} \\ - 12H_{j-3} + H_{j-4}] = 0. \end{aligned} \quad (2.18)$$

The modified equation corresponding to (2.18) is

$$\partial_t h - \varepsilon \partial_{xx} h = -\frac{\delta^3}{8} \partial_{xxxx} h. \quad (2.19)$$

This shows a numerical dissipation that is third order in δ, in sharp contrast to the upwind case (2.10), which has a first-order numerical dissipation. The van Leer scheme will have the correct parabolic behavior when $|\xi|^2 \delta^3 \ll \varepsilon$, where ξ is the wave number. However, when $|\xi|^2 \delta^3 \gg \varepsilon$ the numerical dissipation will dominate the physical dissipation of order ε. Hence, the van Leer scheme does not give the correct parabolic behavior in this regime.

2.4. *The Piecewise Parabolic Method (PPM)*

While the van Leer scheme uses piecewise linear functions to interpolate values for $U_{j+1/2}$ from the cell-average values u_j, the PPM scheme uses piecewise parabolic functions [10]. Specifically, by approximating u with a piecewise parabolic function that for x in the j^{th} cell $[x_{j-1/2}, x_{j+1/2}]$ takes the form

$$U_j(x) = U_j + m_j(x - x_j) + a_j[(x - x_j)^2 - \tfrac{1}{12}\delta^2].$$

Here $U_j(x)$ is defined such that its average over the jth cell equals U_j. Both m_j and a_j can be determined by requiring that the average of $U_j(x)$ over $(j-1)$th and $(j+1)$th cells be U_{j-1} and U_{j+1}, respectively. For a uniform grid these conditions give

$$m_j = \frac{U_{j+1} - U_{j-1}}{2\delta}, \quad a_j = \frac{U_{j+1} - 2U_j + U_{j-1}}{2\delta^2}. \tag{2.20}$$

Higher order formulas are often used to construct m_j and a_j [10], but Eqs. (2.20) are sufficient to convey the general behavior of many PPM schemes. Just as for the van Leer scheme, the monotonicity and convexity of the solution can be preserved by applying constraints on m_j and a_j. We choose slope and convexity limiters for the PPM scheme that accommodate local extrema without sacrificing accuracy and, in so doing, we adopt a bit of the ENO viewpoint [21].

For the telegraph equations (2.1) the above procedure is applied to each member of the diagonalized system (2.5) to obtain

$$\begin{aligned}(W+H)_{j+1/2} &= W_j + H_j + m_j^+(x_{j+1/2} - x_j) \\ &\quad + a_j^+[(x_{j+1/2} - x_j)^2 - \tfrac{1}{12}\delta^2], \\ (W-H)_{j+1/2} &= W_{j+1} - H_{j+1} + m_{j+1}^-(x_{j+1/2} - x_{j+1}) \\ &\quad + a_{j+1}^-[(x_{j+1/2} - x_{j+1})^2 - \tfrac{1}{12}\delta^2],\end{aligned} \tag{2.21}$$

where the superscripts + and − on m and a are associated with quantities $W + H$ and $W - H$, respectively. If the solution resolved by the grid then the flux-limiters do not take effect and $m_j^\pm$ and $a_j^\pm$ are defined by (2.20) with $U = W \pm H$. Consequently, solving (2.21) for $H_{j+1/2}$ and $W_{j+1/2}$ and inserting them into the conservation form (2.4) gives

$$\partial_t H_j + \frac{H_{j+2} - 4H_{j+1} + 6H_j - 4H_{j-1} + H_{j-2}}{12\delta} + \frac{-W_{j+2} + 8W_{j+1} - 8W_{j-1} + W_{j-2}}{12\delta} = 0, \tag{2.22a}$$

$$\partial_t W_j + \frac{W_{j+2} - 4W_{j+1} + 6W_j - 4W_{j-1} + W_{j-2}}{12\delta} + \frac{-H_{j+2} + 8H_{j+1} - 8H_{j-1} + H_{j-2}}{12\delta} = -\frac{1}{\varepsilon} W_j. \tag{2.22b}$$

The modified equations corresponding to this scheme are

$$\begin{aligned}\partial_t h + \partial_x w &= \frac{\delta^3}{12}\partial_{xxxx} h + \frac{\delta^4}{30}\partial_{xxxxx} w, \\ \partial_t w + \partial_x h &= -\frac{1}{\varepsilon} w - \frac{\delta^3}{12}\partial_{xxxx} w + \frac{\delta^4}{30}\partial_{xxxxx} h.\end{aligned} \tag{2.23}$$

This shows the third-order accuracy of this PPM scheme for the telegraph equations (2.1) while holding ε fixed, which is, not unexpectedly, one order better than for the van Leer scheme. This shows that the PPM is less dispersive than the van Leer. However, the dissipation is of the same order as that of van Leer, although with a slightly smaller coefficient.

The behavior of this scheme for small ε while holding δ fixed is as follows. Upon assuming only long wavelengths survive, the flux-limiting can be neglected and Eq. (2.22b) gives

$$W_j = -\varepsilon \frac{-H_{j+2} + 8H_{j+1} - 8H_{j-1} + H_{j-2}}{12\delta} + O(\varepsilon^2),$$

which when substituted into (2.22a) and dropping $O(\varepsilon^2)$ terms yields

$$\begin{aligned}\partial_t H_j &+ \frac{H_{j+2} - 4H_{j+1} + 6H_j - 4H_{j-1} + H_{j-2}}{12\delta} \\ &- \varepsilon \frac{1}{(12\delta)^2}[H_{j+4} - 16H_{j+3} + 64H_{j+2} \\ &+ 16H_{j+1} - 130H_j + 16H_{j-1} + 64H_{j-2} \\ &- 16H_{j-3} + H_{j-4}] = 0.\end{aligned}$$

The modified equation corresponding to this discretization of the heat equation is

$$\partial_t h - \varepsilon \partial_{xx} h = -\frac{\delta^3}{12}\partial_{xxxx} h. \tag{2.24}$$

This shows a numerical dissipation that is third order in δ. Although the PPM scheme is third order by (2.23) while the van Leer scheme is second order by (2.17), comparing (2.19) with (2.24) shows the long-time behavior of both methods to be accurate to third order. Because the numerical dissipation coefficient of the PPM scheme is smaller than that of the van Leer scheme, one may expect that the PPM scheme is slightly less dissipative than the van Leer scheme. Just as with the van Leer scheme, when $|\xi|^2\delta^3 \gg \varepsilon$ the numerical dissipation will dominate the physical dissipation of order ε. Hence, the PPM scheme also does not give the correct long-time behavior in this regime.

2.5. *The Piecewise Steady Approximation*

A particularly effective way to compute the steady state solution of hyperbolic conservation laws with source terms has been to use piecewise steady interpolants over each cell rather than the piecewise constant interpolants of the upwind scheme [14, 40, 45]. A steady state for the telegraph equations written in the diagonalized form (2.5) satisfies

$$\partial_x(w \pm h) = \mp \frac{1}{\varepsilon} w. \tag{2.25}$$

If, instead of using the van Leer slope (2.13), one uses the slope from this steady state equation in the van Leer interpolant (2.11), the upwind determination of the nodal values (2.14) selects

$$(W+H)_{j+1/2} = W_j + H_j - \frac{\delta}{2\varepsilon} W_j,$$
$$(W-H)_{j+1/2} = W_{j+1} - H_{j+1} - \frac{\delta}{2\varepsilon} W_{j+1},$$

which yields

$$H_{j+1/2} = \frac{H_j + H_{j+1}}{2} - \left(1 - \frac{\delta}{2\varepsilon}\right)\frac{W_{j+1} - W_j}{2},$$
$$W_{j+1/2} = -\frac{H_{j+1} - H_j}{2} + \left(1 - \frac{\delta}{2\varepsilon}\right)\frac{W_j + W_{j+1}}{2}.$$

With this flux, the discrete equation (2.4) gives the scheme

$$\partial_t H_j - \frac{H_{j+1} - 2H_j + H_{j-1}}{2\delta} + \left(1 - \frac{\delta}{2\varepsilon}\right)\frac{W_{j+1} - W_{j-1}}{2\delta} = 0, \tag{2.26a}$$

$$\partial_t W_j - \left(1 - \frac{\delta}{2\varepsilon}\right)\frac{W_{j+1} - 2W_j + W_{j-1}}{2\delta} + \frac{H_{j+1} - H_{j-1}}{2\delta} = -\frac{1}{\varepsilon} W_j. \tag{2.26b}$$

The steady state solution of this finite difference system is clearly a second-order approximation of the steady state equation (2.25).

Although one can again use the asymptotic analysis combined with the modified analysis described above to study the parabolic behavior of this scheme, which turns out to be rather lengthy in this case, it is more convenient to employ the discrete Fourier analysis here. Upon substituting

$$H_j = \hat{H}_j e^{-\Lambda t + i\xi j\delta}, \quad W_j = \hat{W}_j e^{-\Lambda t + i\xi j\delta}$$

into (2.26), one finds

$$\Lambda = \Lambda_\pm \equiv \frac{2}{\delta}\sin^2\left(\frac{\xi\delta}{2}\right) + \frac{1}{2\varepsilon}\cos^2\left(\frac{\xi\delta}{2}\right) \pm \frac{1}{2\varepsilon}\cos^2\left(\frac{\xi\delta}{2}\right)\sqrt{1 + \varepsilon\frac{8}{\delta}\tan^2\left(\frac{\xi\delta}{2}\right) - \varepsilon^2\left(\frac{4}{\delta}\right)^2\tan^2\left(\frac{\xi\delta}{2}\right)},$$

and

$$\frac{i}{\delta}\sin(\xi\delta)\left(1 - \frac{\delta}{2\varepsilon}\right)\hat{W}_\pm = \left(\frac{2}{\delta}\sin^2\left(\frac{\xi\delta}{2}\right) - \Lambda_\pm\right)\hat{H}_\pm.$$

As ε tends to 0 while holding ξ fixed, one sees that

$$\Lambda_+ = \frac{4}{\delta}\sin^2\left(\frac{\xi\delta}{2}\right) + \frac{1}{\varepsilon}\cos^2\left(\frac{\xi\delta}{2}\right) + O(\varepsilon),$$
$$\Lambda_- = \varepsilon\left(\left(\frac{2}{\delta}\right)^2\sin^2\left(\frac{\xi\delta}{2}\right) + \left(\frac{4}{\delta}\right)^2\frac{\sin^4(\xi\delta/2)}{\cos^2(\xi\delta/2)}\right) + O(\varepsilon^2). \tag{2.27}$$

Clearly the parabolic behavior of the scheme can be observed by the consistency between Λ_- in (2.27) and λ_- in (2.3). Thus the piecewise steady approximation has the correct parabolic behavior.

In the intermediate regime, when $\varepsilon \sim \delta$, one can also show that the piecewise steady approximation also approximates the equilibrium equation accurately. Use $\delta = \varepsilon Pe$ for fixed Pe. By applying this in (2.26), one can obtain the following modified equations

$$\partial_t h + \left(1 - \frac{Pe}{2}\right)\partial_x w - \frac{\delta}{2}\partial_{xx} h = 0, \tag{2.28a}$$

$$\partial_t w + \partial_x h - \frac{\delta}{2}\left(1 - \frac{Pe}{2}\right)\partial_{xx} w = -\frac{1}{\varepsilon} w. \tag{2.28b}$$

As $\varepsilon \to 0$, (2.28b) gives $w = -\varepsilon\partial_x h + O(\varepsilon^2)$, which applied to (2.28a) gives

$$\partial_t h - \varepsilon\left(1 - \frac{Pe}{2}\right)\partial_{xx} h - \frac{\delta}{2}\partial_{xx} h = 0. \tag{2.29}$$

Equation (2.29) clearly recovers (2.2) since $\delta = \varepsilon$Pe. Thus, in the intermediate regime the piecewise steady approximation also captures the correct parabolic behavior given by the heat equation (2.2).

2.6. *A Modified Upwind Scheme*

In this subsection we show that upwind schemes can be modified in another way so as to capture the proper parabolic behavior. The idea is again to build into the numerical schemes the asymptotics that lead from the hyperbolic system to the parabolic equation, similar to the piecewise steady approximation, but in an implicit way. Here we implement our idea by modifying the basic upwind scheme and leave the modification of higher order Godunov schemes to the next two sections, where more general nonlinear 2×2 systems are treated.

Note that the asymptotic balance that leads from the hyperbolic telegraph equations (2.1) to the heat equation in (2.2) is

$$\partial_x h = -(1/\varepsilon) w. \tag{2.30}$$

If ε is small and w is at least order ε then the gradient of h may not be neglected. However, the upwind scheme (2.6) ignored this variation in h, approximating it as a constant throughout each cell. A first cut at incorporating this variation into the scheme may be made by approximating H_j and H_{j+1} by a Taylor expansion about the node $x = x_{j+1/2}$, which, using (2.30), leads to

$$\begin{aligned} H_j &\sim H_{j+1/2} + \frac{\delta}{2\varepsilon} W_{j+1/2}, \\ H_{j+1} &\sim H_{j+1/2} - \frac{\delta}{2\varepsilon} W_{j+1/2}. \end{aligned} \tag{2.31}$$

Here we expand the cell-average values in terms of the nodal values, a critical difference from the piecewise steady approximation, which does the opposite. By using (2.31), the upwind selection becomes

$$W_j + H_j = W_{j+1/2} + H_{j+1/2} + \frac{\delta}{2\varepsilon} W_{j+1/2}, \tag{2.32a}$$

$$W_{j+1} - H_{j+1} = W_{j+1/2} - H_{j+1/2} + \frac{\delta}{2\varepsilon} W_{j+1/2}. \tag{2.32b}$$

Upon solving (2.32) for $H_{j+1/2}$ and $W_{j+1/2}$ and substituting them into the conservation form (2.4) gives the modified upwind scheme

$$\partial_t H_j - \frac{H_{j+1} - 2H_j + H_{j-1}}{2\delta + \delta^2/\varepsilon} + \frac{W_{j+1} - W_{j-1}}{2\delta + \delta^2/\varepsilon} = 0, \tag{2.33a}$$

$$\partial_t W_j - \frac{W_{j+1} - 2W_j + W_{j-1}}{2\delta} + \frac{H_{j+1} - H_{j-1}}{2\delta} = -\frac{1}{\varepsilon} W_j. \tag{2.33b}$$

The modified equations corresponding to this scheme are

$$\begin{aligned} \partial_t h + \frac{2\delta}{2\delta + \delta^2/\varepsilon} \partial_x w - \frac{\delta^2}{2\delta + \delta^2/\varepsilon} \partial_{xx} h = 0, \\ \partial_t w + \partial_x h - \frac{\delta}{2} \partial_{xx} w = -\frac{1}{\varepsilon} w. \end{aligned}$$

For fixed ε, this is clearly a first-order discretization of the telegraph equations (2.1).

If ε is small, then for fixed δ, Equation (2.33b) gives

$$W_j = -\varepsilon \frac{H_{j+1} - H_{j-1}}{2\delta} + O(\varepsilon^2),$$

while (2.33a) becomes

$$\partial_t H_j - \varepsilon \frac{H_{j+1} - 2H_j + H_{j-1}}{\delta^2} = O\left(\frac{\varepsilon^2}{\delta}\right).$$

This is an approximation to the equilibrium heat equation (2.2) with an accuracy of $O(\varepsilon^2/\delta)$. Thus the modified upwind scheme has the correct parabolic behavior with a coarse grid. One may expect that coarse grids independent of ε can be used to capture the parabolic behavior described by (2.2).

In the intermediate regime, when $\varepsilon \sim \delta$, one can also show that the modified equation approximates the equilibrium equation accurately. Let $\delta = \varepsilon$ Pe for fixed Pe. By applying this in (2.33), one sees that (2.33) approximates

$$\partial_t h + \frac{2}{2 + \text{Pe}} \partial_x w - \frac{\varepsilon\,\text{Pe}}{2 + \text{Pe}} \partial_{xx} h = 0, \tag{2.34a}$$

$$\partial_t w + \partial_x h - \frac{\delta}{2} \partial_{xx} w = -\frac{1}{\varepsilon} w. \tag{2.34b}$$

As $\varepsilon \to 0$, (2.34b) gives $w = -\varepsilon\, \partial_x h + O(\varepsilon^2)$, which applied to (2.34a) gives

$$\partial_t h - \frac{2\varepsilon}{2 + \text{Pe}} \partial_{xx} h - \frac{\varepsilon\,\text{Pe}}{2 + \text{Pe}} \partial_{xx} h = O(\varepsilon^2),$$

or

$$\partial_t h - \varepsilon\, \partial_{xx} h = O(\varepsilon^2).$$

Thus, in the intermediate regime the modified upwind scheme again captures the correct parabolic behavior given by the heat equation (2.2).

2.7. *Numerical Results*

In all the numerical examples presented in this article we have always chosen $\Delta t \ll \tau$ so that it is small enough that our analysis will not be affected by the error introduced by the time discretization. We will only present the numerical results for H. The behavior of W is similar under the resolved time discretization. Fully discrete numerical schemes are studied in a forthcoming paper [24].

Here we test the above five schemes for the linear telegraph equations (2.1), with $c = 1$, over the periodic interval $0 \le x \le 2$ with initial condition $h(0, x) = 2 + \sin(\pi x)$ and $w(0, x) = -0.1$. We take $\varepsilon = 0.01$. Figure 1 shows the results of the "exact" solution and the numerical solutions computed with the five schemes (for short, we use UW for the upwind scheme, vL for the van Leer scheme, PPM for the PPM method, PS for the piecewise steady approximations, and MUW for the modified upwind scheme) discussed earlier. The "exact" solution is computed by PPM on a fine grid with $\delta = 0.001$, corresponding to

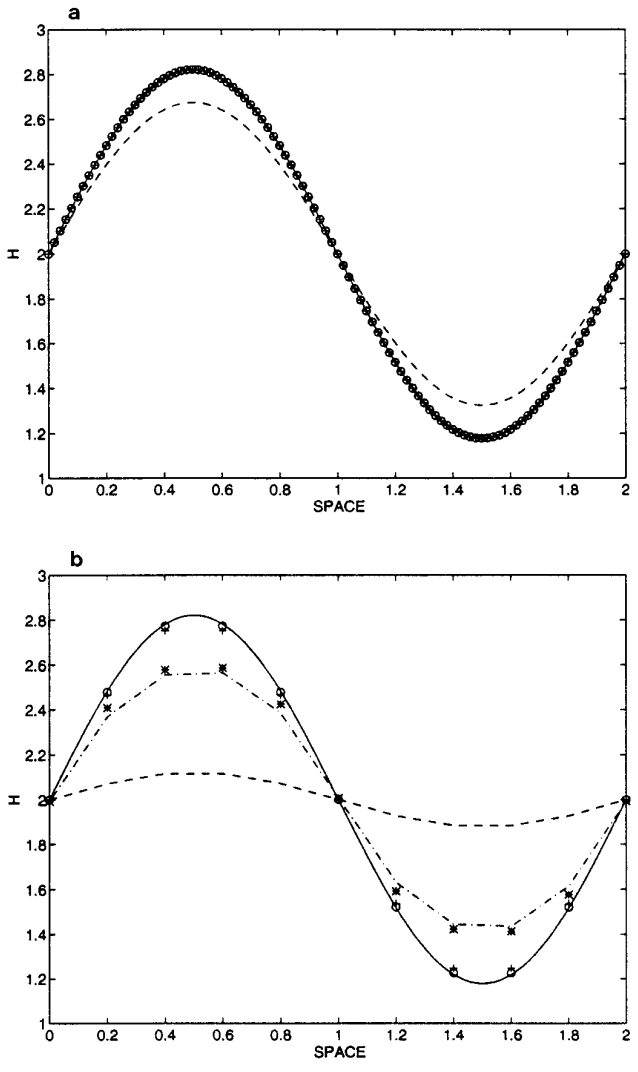

FIG. 1. Numerical solutions of Eqs. (2.1) at $t = 2$ for $\varepsilon = 0.01$. Our "exact" solution (the solid line) is obtained by PPM with $\delta = 0.001$. (a) Numerical solutions are obtained with an intermediate grid size $\delta = 0.01$ (Pe = 1) and plotted by dashed line for UW, "+" for PS, and "o" for MUW, respectively. (b) Numerical solutions are obtained with a coarse grid size $\delta = 0.1$ (Pe = 10) and plotted by dashed line for UW, "–·" for vL, "*" for PPM, "+" for PS, and "o" for MUW, respectively.

Pe = 0.1. The coarse grids use $\delta = 0.1$ (Pe = 10). We also take $\delta = \varepsilon = 0.01$ (Pe = 1) to compute the problem in the intermediate regime. We output the solutions at $t = 2$.

In the intermediate regime vL and PPM work fine, in agreement with the fact that their numerical dissipations are of order δ^3, much smaller than the physical dissipation of order ε. Thus we only plot the "exact" solution, the solutions of UW, PS, and MUW in Fig. 1a. It can be seen that UW decays at an unphysical rate. This agrees with our earlier analysis in which it is shown that the upwind scheme has a numerical dissipation of order δ, which is in the same order as the physical dissipation rate in the intermediate regime. The MUW and PS give accurate numerical solutions in this regime, as predicted by our analysis. In Fig. 1b, we plot the numerical solutions for all five schemes discussed earlier in the coarse regimes. All except the MUW and PS give bad results, showing the domination of the numerical dissipation on these coarse grids. One can also see that UW gives a much worse result than vL and PPM; PPM gives slightly better result than vL; and MUW is slightly better than PS. These numerical results all agree with our results using the asymptotic analysis and the modified equation analysis.

3. CONVECTION WITH DIFFUSION: A MODEL

In general, solutions of hyperbolic systems with stiff relaxation terms exhibit long-time behavior governed by a convection–diffusion system, not just a diffusion system such as was studied in the last section. As an illustrative model we consider the 2×2 p-system with relaxation (1.3):

$$\partial_t h + \partial_x w = 0, \tag{3.1a}$$

$$\partial_t w + \partial_x p(h) = -(1/\tau)(w - f(h)). \tag{3.1b}$$

Provided that the stability condition (1.5) is satisfied, the long-time behavior of its solution is governed by (1.4):

$$\partial_t h + \partial_x f(h) = \tau \partial_x [(p'(h) - f'(h)^2)\partial_x h], \tag{3.2a}$$

$$w = f(h) - \tau(p'(h) - f'(h)^2)\partial_x h. \tag{3.2b}$$

When system (3.1) is compared with the telegraph equations (2.1) of the last section one sees that, in addition to the obvious new feature of nonlinearity, there is the appearance of a convective term in the parabolic equation (3.2a). Indeed, this term gives the leading order dynamics of solutions of the system (3.1) once the local equilibrium $w = f(h)$ is approximately established after a time scale of τ. The hyperbolic nature of the convective term in (3.2a) gives rise to solutions that may contain large gradients (viscous shocks). It is clear that any numerical scheme for (3.1) that hopes to compute into such regimes must give a good discretization of this term. The diffusive term in (3.2a) becomes important over time scales that are $O(1/\varepsilon)$, compared to those associated with the convective term. The numerical scheme for (3.1) must therefore become a good discretization of that term, too, if one hopes to compute solutions of (3.1) accurately for very long times.

3.1. *Discrete Long-Time Behavior: A Linear Model*

In Section 2 we have analyzed the long-time, parabolic behavior of several numerical schemes. When similar analysis is performed for the discretization of (3.1), it is also necessary to understand how the discretization approxi-

mates the convection term $\partial_x f(h)$ when passing to the parabolic description. This will first be illustrated for the linear model

$$\begin{aligned} \partial_t h + \partial_x w &= 0, \\ \partial_t w + c^2 \partial_x h &= -(1/\tau)(w - bh), \end{aligned} \tag{3.3}$$

where we assume that $\tau > 0$ and $0 < |b| < c$. The long-time behavior of its solutions is governed by the linear convection–diffusion equation

$$\partial_t h + b\partial_x h = \tau(c^2 - b^2)\partial_{xx} h. \tag{3.4}$$

Of course, our observations will naturally apply to the fully nonlinear model (3.1).

When the upwind scheme (2.7) is applied to (3.3) and analyzed as $\mathrm{Pe} \to \infty$ as we did in the last section, the long-time behavior of its solutions is found to be governed by

$$\begin{aligned} \partial_t H_j + b\frac{H_{j+1} - H_{j-1}}{2\,\Delta x} &= c\frac{H_{j+1} - 2H_j + H_{j-1}}{2\,\Delta x} \\ &\quad + \tau(c^2 - b^2)\frac{H_{j+2} - 2H_j + H_{j-2}}{(2\,\Delta x)^2}. \end{aligned} \tag{3.5}$$

This approximates the advection term $b\partial_x h$ in (3.4) with a central difference plus a first-order numerical dissipation with a viscosity coefficient of $c(\Delta x/2)\partial_{xx} h$. Indeed, an upwind scheme applied directly to

$$\partial_t h + b\partial_x h = 0,$$

which is (3.4) without the diffusion term, would give the difference equation

$$\partial_t H_j + b\frac{H_{j+1} - H_{j-1}}{2\,\Delta x} = |b|\frac{H_{j+1} - 2H_j + H_{j-1}}{2\,\Delta x}. \tag{3.6}$$

If one compares (3.6) with (3.5) (without the last term) then one finds that discretization (3.5) of Eq. (3.4) contains more numerical dissipation (having a viscosity coefficient of $c\,\Delta x/2$) than the upwind scheme (3.6) (having a viscosity coefficient of $|b|\Delta x/2$, where $|b| < c$).

Similarly, the long-time behavior associated with the van Leer scheme for (3.3) is governed by

$$\begin{aligned} \partial_t H_j + b\frac{-H_{j+2} + 6H_{j+1} - 6H_{j-1} + H_{j-2}}{8\,\Delta x} \\ = -c\frac{H_{j+2} - 4H_{j+1} + 6H_j - 4H_{j-1} + H_{j-2}}{8\,\Delta x} \\ + \tau(c^2 - b^2)\frac{1}{8\,\Delta x^2}[H_{j+4} - 12H_{j+3} + 36H_{j+2} \\ + 12H_{j+1} - 74H_j + 12H_{j-1} + 36H_{j-2} \\ - 12H_{j-3} + H_{j-4}]. \end{aligned} \tag{3.7}$$

This is a second-order approximation to the parabolic equation (3.4). This long-time numerical approximation, like the upwind scheme, is more dissipative than the second-order upwind (van Leer) scheme applied directly to (3.4).

The long-time behavior associated with the PPM scheme for (3.3) is governed by

$$\begin{aligned} \partial_t H_j + b\frac{-H_{j+2} + 8H_{j+1} - 8H_{j-1} + H_{j-2}}{12\,\Delta x} \\ = -c\frac{H_{j+2} - 4H_{j+1} + 6H_j - 4H_{j-1} + H_{j-2}}{12\,\Delta x} \\ + \tau(c^2 - b^2)\frac{1}{12\,\Delta x^2}[H_{j+4} - 16H_{j+3} + 64H_{j+2} \\ + 16H_{j+1} - 130H_j + 16H_{j-1} + 64H_{j-2} \\ - 16H_{j-3} + H_{j-4}]. \end{aligned}$$

Therefore, due to the presence of the stiff relaxation term in (3.3), these upwind type schemes at the relaxation level do not agree with the upwind schemes to the reduced parabolic equation (3.4). Similar observations were made by Pember [39]. Also, if one uses coarse grids, the leading numerical dissipation, as discussed for the telegraph equations, may dominate the physical dissipation.

3.2. *A Modified Flux for the Nonlinear Model*

We seek robust schemes for these problems that possess the following properties. First, in the nonstiff regime they should be a high-order shock-capturing scheme that can properly capture the discontinuous features of the solution. The higher order Godunov schemes are already extremely well suited for this task. Second, when the relaxation term becomes stiff, these schemes should have a long-time behavior that are consistent and stable discretizations to the convection–diffusion equation. Moreover, we want the long-time convection discretization to be also a Godunov type scheme to the reduced convection term. Similar attempts were made in [39]. Third, in the regime where the parabolic term becomes important (over the longer time scale), the schemes should capture the correct long-time behavior, just as discussed in the last section.

More specifically, we seek the long-time approximation of (3.2a) in the form

$$\partial_t H_j + \frac{f(H_{j+1/2}) - f(H_{j-1/2})}{\Delta x} = \frac{\tau}{\Delta x^2}(p'(H_{j+1/2}) - f'(H_{j+1/2})^2)(H_{j+1} - H_j) - \frac{\tau}{\Delta x^2}(p'(H_{j-1/2}) - f'(H_{j-1/2})^2)(H_j - H_{j-1}), \tag{3.8}$$

where the edge fluxes $H_{j+1/2}$ are defined by a higher order Godunov scheme (vL or PPM say) through the solution of the Riemann problem of the leading hyperbolic convection equation

$$\partial_t h + \partial_x f(h) = 0. \tag{3.9}$$

It is clear that (3.8) is a good approximation of the nonlinear convection–diffusion equation (3.2a); the main question is how a numerical scheme for (3.1) can pass to the scheme (3.8).

Suppose the numerical scheme for (3.1) has the form

$$\partial_t H_j + \frac{W^{(1)}_{j+1/2} - W^{(1)}_{j-1/2}}{\Delta x} = 0, \tag{3.10a}$$

$$\partial_t W_j + \frac{p(H^{(1)}_{j+1/2}) - p(H^{(1)}_{j-1/2})}{\Delta x} = -\frac{1}{\tau}(W_j - f(H_j)), \tag{3.10b}$$

where the edge values $W^{(1)}_{j+1/2}$ and $H^{(1)}_{j+1/2}$ are defined by higher order Godunov schemes using the solution of the Riemann problem of the p-system,

$$\begin{aligned} \partial_t h + \partial_x w &= 0, \\ \partial_t w + \partial_x p(h) &= 0. \end{aligned} \tag{3.11}$$

Left unmodified, as $\mathrm{Pe} \to \infty$, the solutions of this scheme will behave like those of a central-difference scheme for (3.2a) just as described through the linear model. Rather, we wish to modify the edge values so that the solutions behave like those of the differencing scheme (3.8).

We propose to incorporate the asymptotic behavior of w in (3.2b) into the new nodal values through the simple interpolation

$$\begin{aligned} W_{j+1/2} &= a_{j+1/2} W^{(1)}_{j+1/2} + (1 - a_{j+1/2}) W^{(2)}_{j+1/2}, \\ H_{j+1/2} &= H^{(1)}_{j+1/2}, \end{aligned} \tag{3.12}$$

where $W^{(2)}_{j+1/2}$ is the numerical analog of (3.2b) given by

$$W^{(2)}_{j+1/2} = f(H^{(2)}_{j+1/2}) + \frac{\tau}{\Delta x}(p'(H^{(2)}_{j+1/2}) - f'(H^{(2)}_{j+1/2})^2)(H_{j+1} - H_j), \tag{3.13}$$

and $H^{(2)}_{j+1/2}$ is defined by the same higher order Godunov schemes based on the solution of the Riemann problem of (3.9). The weight function $a_{j+1/2} = a(\mathrm{Pe})$ introduced in (3.12) lies between 0 and 1 and will be chosen to depend on the local Peclet number $\mathrm{Pe} = \Delta x / c\tau$, where $c = c_{j+1/2}$ is the local maximal characteristic speed of (3.1):

$$c_{j+1/2} = \sqrt{p(H^{(1)}_{j+1/2})}. \tag{3.14}$$

For this modified set of nodal values, the numerical flux for system (3.1) becomes

$$\begin{aligned} W_{j+1/2} &= a_{j+1/2} W^{(1)}_{j+1/2} + (1 - a_{j+1/2}) f(H^{(2)}_{j+1/2}) \\ &\quad + (1 - a_{j+1/2}) \frac{\tau}{\Delta x}(p'(H^{(2)}_{j+1/2}) \\ &\quad - f'(H^{(2)}_{j+1/2})^2)(H_{j+1} - H_j), \\ H_{j+1/2} &= H^{(1)}_{j+1/2}. \end{aligned} \tag{3.15}$$

Such an approach is a generalization of the piecewise steady approximation and the modified upwind scheme. We will abbreviate this scheme as MvL if $H^{(1)}_{j+1/2}$, $H^{(2)}_{j+1/2}$, $W^{(1)}_{j+1/2}$ and $W^{(2)}_{j+1/2}$ are defined by the van Leer flux, and MPPM if they are defined by the PPM flux. The weight factor $a(\mathrm{Pe})$ should be such that when the Pe is small (for fine grid), it recovers the higher order Godunov scheme (3.10); when the Pe is large (coarse grid) it leads to scheme (3.8). So at a minimum, it is natural to require

$$\lim_{\mathrm{Pe}\to 0} a(\mathrm{Pe}) = 1; \quad \lim_{\mathrm{Pe}\to\infty} a(\mathrm{Pe}) = 0. \tag{3.16}$$

In so doing, the fluxes defined in (3.15) yield correct asymptotic properties for both fine and coarse grids.

Because there are many choices of a that satisfy these conditions, a good choice will be one such that in the intermediate regime when $\mathrm{Pe} \sim 1$ the asymptotic behavior of scheme (3.15) approximates system (3.2) as accurately as possible. In order to find an appropriate form for a we apply flux (3.15) to solve the linear system (3.3).

For example, applying the MvL to the linear system (3.3), one can obtain the following long-time behavior when $\mathrm{Pe} = \Delta x / c\tau \to \infty$ (without loss of generality we assume that $b > 0$ here):

$$\partial_t H_j + ab\frac{-H_{j+2} + 6H_{j+1} - 6H_{j-1} + H_{j-2}}{8\Delta x} + (1 - a)b\frac{H_{j+1} + 3H_j - 5H_{j-1} + H_{j-2}}{4\Delta x} = -ac\frac{H_{j+2} - 4H_{j+1} + 6H_j - 4H_{j-1} + H_{j-2}}{8\Delta x}$$

$$+ a\tau(c^2 - b^2)\frac{1}{8\Delta x^2}[H_{j+4} - 12H_{j+3} + 36H_{j+2} + 12H_{j+1} - 74H_j + 12H_{j-1} + 36H_{j-2} - 12H_{j-3} + H_{j-4}] + (1-a)\tau(c^2 - b^2)\frac{H_{j+1} - 2H_j + H_{j-1}}{(\Delta x)^2}.$$

This discretization has the modified equation

$$\partial_t h + b\partial_x h = \tau(c^2 - b^2)\partial_{xx}h - \tfrac{1}{8}ac(\Delta x)^3\partial_{xxxx}h - \tfrac{1}{12}\tau(1-a)(c^2-b^2)(\Delta x)^2\partial_{xxxx}h \tag{3.17}$$

after ignoring the dispersive errors and other higher order terms. (The MPPM gives a similar modified equation modulo a different dispersion error and some constant coefficients). Here we have ignored higher order terms, as well as the third order, dispersive terms since our goal is to eliminate the unphysical numerical dissipation instead of the numerical dispersion error. We want to choose a so that the numerical dissipation (the second and third terms in the right side of (3.17)) becomes much smaller than the physical dissipation $\tau(c^2 - b^2)\partial_{xx}h$. Because the last term in (3.17) is in the order of $\tau(\Delta x)^2$, which has a higher order than the physical dissipation term appearing in the first term of the right side of (3.17), the best one can do is to match the order of the second term on the right of (3.17) with the last term. So we set

$$ac(\Delta x)^3\partial_{xxxx}h \sim \tau(1-a)(c^2-b^2)(\Delta x)^2\partial_{xxxx}h.$$

Because $0 \le a \le 1$, a choice of a will be

$$a \sim \frac{c\tau}{\Delta x} = \frac{1}{\mathrm{Pe}}. \tag{3.18}$$

Roughly speaking, a should depend linearly on the reciprocal of Pe. A good candidate that depends smoothly on Pe is

$$a = \tanh(1/\mathrm{Pe}), \tag{3.19}$$

because

$$\tanh\left(\frac{1}{\mathrm{Pe}}\right) = \frac{1}{\mathrm{Pe}} + O\left(\frac{1}{\mathrm{Pe}^3}\right), \quad \text{if Pe} \gg 1;$$
$$\left|\tanh\left(\frac{1}{\mathrm{Pe}}\right) - 1\right| \le 2\exp\left(-\frac{2}{\mathrm{Pe}}\right), \quad \text{if Pe} \ll 1. \tag{3.20}$$

With this choice of a the numerical dissipation becomes of order $c^2\tau(\Delta x)^2$ *uniformly* in Δx and τ so the physical dissipation always dominates. Also it can be observed from (3.15) and (3.20) that, as one increases Pe, the scheme (3.15) becomes a better approximation to difference scheme (3.8) for (3.2a). So for the weakly nonlinear regime one just needs cells fine enough to maintain the accuracy of (3.8) without worrying about τ.

We should point out that the linear interpolation (3.12) might not be the optimal choice. It is still an open question to determine the best way to incorporate the two numerical fluxes [39]. However, we believe that the linear interpolation is a reasonable choice. First, it is a convex combination of the two fluxes. If both fluxes are total-variation-diminishing (TVD) or essentially non-oscillatory (ENO) then such a convex combination possesses the TVD or ENO property and no new oscillations should be generated by this interpolation. Second, although one might suspect that the scheme may reduce to a lower order method in the intermediate regime when Pe ~ 1, based on the results in [17] for the linear numerical transport schemes in diffusive regimes, we conjecture that such a modification still maintains a uniform convergence (with respect to Pe) to the solution of the relaxation system (3.1). Third, since the function a rapidly makes the transition from its coarse gird behavior (3.18) to its fine grid value of 1, such an interpolation is of high order accuracy for most values of Pe. The drawback of this interpolation is that in the intermediate regime it may not be an upwind scheme with respect to the local equilibrium equation (3.2a). So far we have not been able to construct a scheme that is upwind for all range of Pe.

3.3. *Numerical Results*

We first examine a problem in the regime where the long-time behavior is important. Consider a p-system over the interval [0, 1] given by

$$\partial_t h + \partial_x w = 0, \tag{3.21a}$$

$$\partial_t w - \partial_x\left(\frac{1}{h^2}\right) = -100(w - 0.01(h-2)^2). \tag{3.21b}$$

Its long-time behavior is described by

$$\partial_t h + 0.01\,\partial_x(h-2)^2 = 0.01\,\partial_x\left[\left(\frac{2}{h^3} - 0.0004(h-2)^2\right)\partial_x h\right], \tag{3.22a}$$

$$w = 0.01(h-2)^2 - 0.01\left(\frac{2}{h^3} - 0.0004(h-2)^2\right)\partial_x h. \tag{3.22b}$$

The initial conditions for this problem are

$$h(0,x) = 2 + \sin(\pi x), \quad w(0,x) = -0.01, \tag{3.23}$$

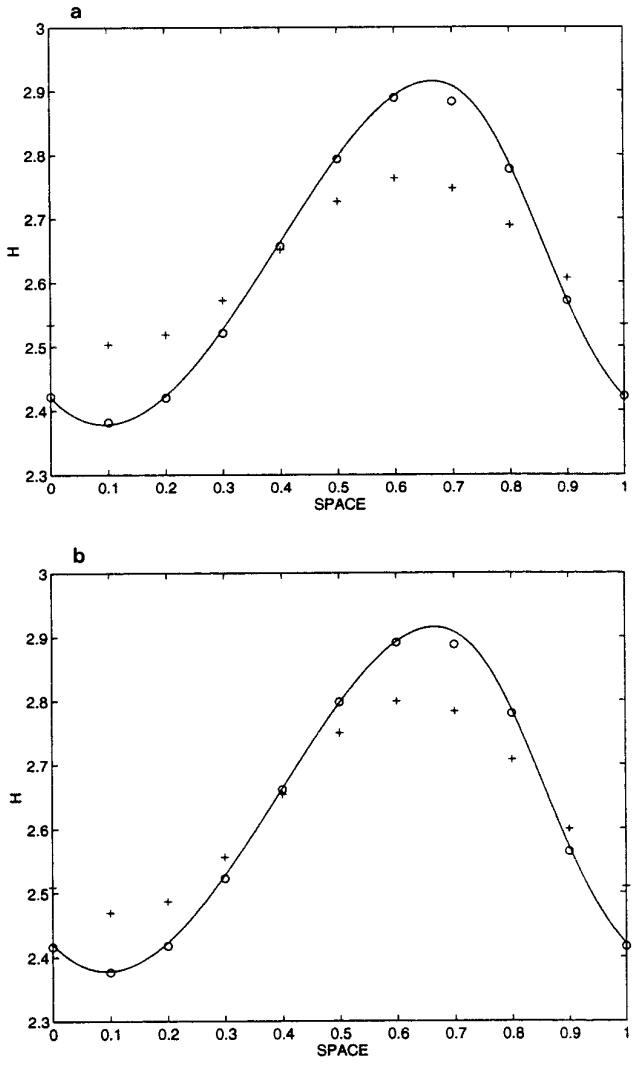

FIG. 2. Comparisons of high order Godunov methods and their modifications with the "exact" solution (solid lines) of (3.21) and (3.23) at $t = 10$ for $\Delta x = 0.1$ and $\tau = 0.01$. In this example Pe ranges between 20 and 36.7423. The "exact" solution is obtained with PPM by taking $\Delta x = 0.001$. Upper: vL (+) and MvL (o) vs exact. Below: PPM (+) and MPPM (o) vs exact.

and the boundary condition is periodic. Here $\tau = 0.01$. The nonlinear convection and the diffusion terms in (3.22a) are of the same order so that the spatial derivatives of the smooth solution should be of order 1. In this problem the maximal characteristic speed $c = \sup\sqrt{2/h^3}$ ranges from 0.2722 to 0.5. We choose $\Delta x = 0.1$; thus Pe ranges from 20 to 36.7423. The results at $t = 10$ are depicted in Fig. 2, with the "exact" solution obtained by PPM with $\Delta x = 0.001$. Both vL and PPM dissipate so fast that they do not capture the correct physical dissipation at all. The MvL and MPPM, however, give a much more accurate dissipation rate in this coarse regime. For smooth solutions, MvL and MPPM give second- and third-order accuracy to the parabolic equation (3.22a). Also PPM (or MPPM) performs slightly better than vL (or MvL) because it is one order higher in accuracy. This example shows that the modified schemes are good in reducing the numerical dissipation in the weakly nonlinear limit with large Pe numbers.

We next test a problem in its strongly nonlinear regime so that the leading convection term dominates, with a thin viscous layer. We would like to see how the modified schemes perform in the intermediate regime where Pe $\sim$ 1. We consider the p-system (3.1) over the interval $[-0.5, 1.5]$ with $p(h) = \frac{1}{2}h^2 + h$ and $f(h) = \frac{1}{2}h^2$:

$$\partial_t h + \partial_x w = 0, \tag{3.24a}$$

$$\partial_t w + \partial_x(\tfrac{1}{2}h^2 + h) = -100(w - \tfrac{1}{2}h^2), \tag{3.24b}$$

The parabolic equation (3.2a) in this case is just

$$\partial_t h + \partial_x(\tfrac{1}{2}h^2) = 0.01\,\partial_x[(1 + h - h^2)\partial_x h]. \tag{3.25}$$

The initial conditions are taken to be

$$h(0,x) = \begin{cases} 1 & \text{for } -0.5 < x < 0.2, \\ 0.2 & \text{for } 0.2 < x < 1.5, \end{cases} \qquad w(0,x) = 0. \tag{3.26}$$

The reflecting boundary conditions are applied. The exact solution to this problem is a shock layer moving to the right with a speed of 0.6. If Pe $\gg$ 1, then all schemes give sharp, underresolved shock profiles without numerical oscillations. The transition across the shock take two to three spatial grid points, which captures only the leading behavior without resolving the viscous layer. In Fig. 3, we choose 150 cells over $[-0.5, 1.5]$. Then Pe ranges between 0.9428 and 1.2172, which is in the intermediate regime. We depict the results at $t = 0.5$ and $t = 1.0$ in $[-0.2, 1]$ to focus on the viscous shock profiles. The "exact" solution was obtained with PPM by taking $\Delta x = 0.001$. All the schemes give comparable results, showing that in the intermediate regimes the MvL and MPPM are quite comparable to their unmodified counterparts. Thus our linear interpolation (3.12) does not seem to downgrade the quality of numerical results even in the intermediate regimes.

4. GENERAL 2 × 2 SYSTEMS AND THE RIVER EQUATIONS

4.1. *General* 2 × 2 *Systems*

In this section we want to show how to generalize the modified Godunov schemes presented in the last section for the 2 × 2 p-system to more general 2 × 2 systems of the form

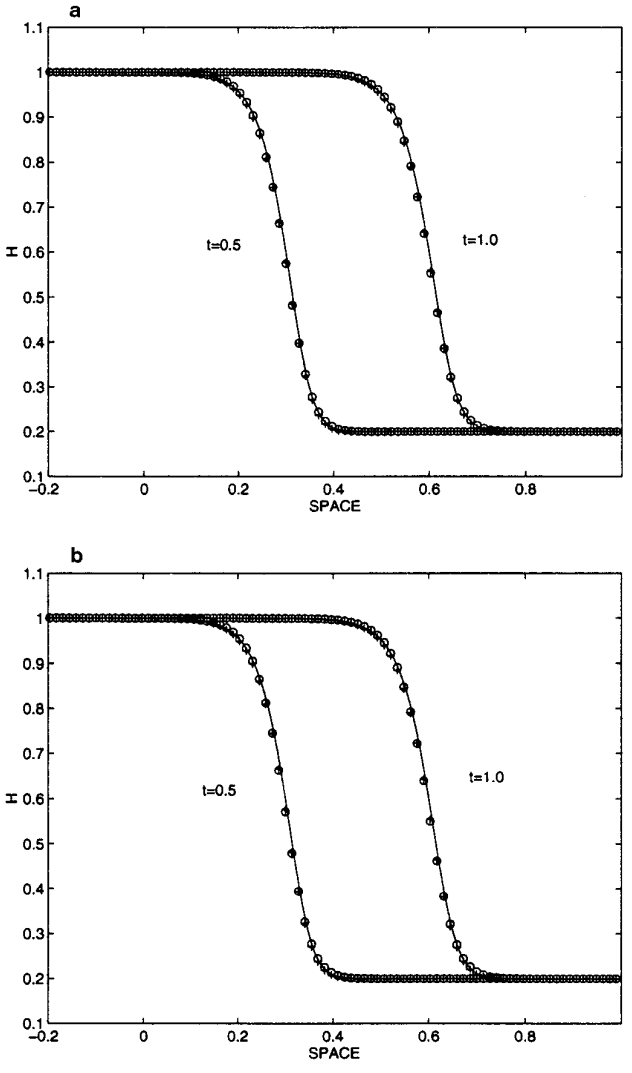

FIG. 3. Comparisons of high-order Godunov methods and their modifications with the "exact" solution (solid lines) of (3.24) and (3.26) at $t = 0.5$ and $t = 1.0$ for $\tau = 0.01$, $\Delta x = 0.0133$. In this example Pe ranges between 0.9428 and 1.2172. The "exact" solution is obtained with PPM by taking $\Delta x = 0.001$. Upper: vL (+) and MvL (o) vs exact. Below: PPM (+) and MPPM (o) vs exact.

$$\partial_t h + \partial_x f_1(h, w) = 0, \tag{4.1a}$$

$$\partial_t w + \partial_x f_2(h, w) = -l(h, w). \tag{4.1b}$$

This system is assumed to be strictly hyperbolic with real and distinct characteristic velocities given by

$$\Lambda_\pm = \tfrac{1}{2}(\partial_h f_1 + \partial_w f_2 \pm \sqrt{(\partial_h f_1 - \partial_w f_2)^2 + 4\partial_w f_1 \partial_h f_2}). \tag{4.2}$$

Assume for each h there exists a unique linearly asymptotically stable equilibrium $w = e(h)$ of the ordinary differential equation obtained by neglecting the spatial derivatives in (4.1b) and holding h fixed. When this is the case, $w = e(h)$ satisfies

$$l(h, e(h)) = 0, \quad \partial_w l(h, e(h)) > 0. \tag{4.3}$$

Furthermore, assume that the two equations in (4.1) are coupled such that

$$\partial_w f_1(h, e(h)) \neq 0. \tag{4.4}$$

Clearly, these assumptions are satisfied when the system (4.1) is specialized to the p-system (1.3) considered previously.

The parabolic approximation for system (4.1) is the scalar convection–diffusion equation [7]

$$\partial_t h + \partial_x f(h) = \partial_x[g(h)\partial_x h], \tag{4.5}$$

with flux $f(h) \equiv f_1(h, e(h))$, and diffusion coefficient

$$g(h) \equiv \left.\frac{\partial_w f_1(\partial_h f_2 - (\partial_h f_1 - \partial_w f_2)e' - \partial_w f_1(e')^2)}{\partial_w l}\right|_{w=e(h)}.$$

The characteristic velocity associated with (4.5) when $\varepsilon = 0$ is

$$\lambda(h) \equiv f'(h) = \partial_h f_1(h, e(h)) + \partial_w f_1(\mathrm{h}, e(h))e'(h),$$

and the stability criterion for (4.5) is

$$\Lambda_-(h, e(h)) \leq \lambda(h) \leq \Lambda_+(h, e(h)), \tag{4.6}$$

where $\Lambda_\pm$ are the characteristic velocities (4.2) of system (4.1). The relation of this condition to the nonnegativity of the diffusion coefficient (4.6) is manifest from the fact [7] that

$$g(h) = \frac{(\Lambda_+(h, e(h)) - \lambda(h))(\lambda(h) - \Lambda_-(h, e(h)))}{\partial_w l(h, e(h))}.$$

Finally, as with system (1.3), a spatially homogeneous equilibrium of the system (4.1) in the form $(h, w) = (\bar{h}, e(\bar{h}))$ for any constant $\bar{h}$ is stable if and only if $h = \bar{h}$ satisfies (4.6).

In this problem the relaxation time τ and the characteristic variable c as

$$\begin{aligned} \tau(h) &= \left.\frac{1}{\partial_w l(h, w)}\right|_{w=e(h)}, \\ c(h) &= \left.\max\{|\Lambda_+(h, w)|, |\Lambda_-(h, w)|\}\right|_{w=e(h)}. \end{aligned} \tag{4.7}$$

The local Peclet number is then

$$\mathrm{Pe}(h) = \frac{\Delta x}{c(h)\tau(h)}. \tag{4.8}$$

Assume that the unmodified numerical scheme for system (4.1) is

$$\begin{aligned} &\partial_t H_j + \frac{f_1(H^{(1)}_{j+1/2}, W^{(1)}_{j+1/2}) - f_1(H^{(1)}_{j-1/2}, W^{(1)}_{j-1/2})}{\Delta x} = 0, \\ &\partial_t W_j + \frac{f_2(H^{(1)}_{j+1/2}, WH^{(1)}_{j+1/2}) - f_2(H^{(1)}_{j-1/2}, WH^{(1)}_{j-1/2})}{\Delta x} \\ &\qquad = -l(H_j, W_j), \end{aligned} \tag{4.9}$$

where the nodal values $H^{(1)}_{j+1/2}$ and $W^{(1)}_{j+1/2}$ are defined by some higher order Godunov scheme based on the Riemann problem of the hyperbolic conservation law

$$\begin{aligned} \partial_t h + \partial_x f_1(h, w) = 0, \\ \partial_t w + \partial_x f_2(h, w) = 0. \end{aligned} \tag{4.10}$$

In order to recover the correct long-time behavior, we modify the scheme (4.9) like we did to get the modified upwind scheme for the p-system. Specifically, let the numerical fluxes be

$$\begin{aligned} f_{1,j+1/2} &= a_{j+1/2} f_1(H^{(1)}_{j+1/2}, W^{(1)}_{j+1/2}) + (1 - a_{j+1/2}) f(H^{(2)}_{j+1/2}) \\ &\quad - \varepsilon(1 - a_{j+1/2}) g(H^{(2)}_{j+1/2})(H_{j+1} - H_j), \end{aligned} \tag{4.11a}$$

$$f_{2,j+1/2} = f_2(H^{(1)}_{j+1/2}, W^{(1)}_{j+1/2}), \tag{4.11b}$$

where the new nodal values $H^{(2)}_{j+1/2}$ are defined by the same kind of Godunov scheme as in (4.9), but using the solution of Riemann problem for the scalar conservation law

$$\partial_t h + \partial_x f(h) = 0. \tag{4.12}$$

In (4.11) a plays the same role as it did for the p-system. In particular, we again choose a to depend on the local Peclet number as

$$a_{j+1/2} = \tanh\left(\frac{1}{\mathrm{Pe}_{j+1/2}}\right), \tag{4.13}$$

where Pe is defined in (4.8) with

$$c_{j+1/2} = c(H^{(1)}_{j+1/2}), \quad \tau_{j+1/2} = \tau(H^{(1)}_{j+1/2}). \tag{4.14}$$

4.2. *Application to the River Equations*

An example of (4.1) system that we will use to numerically test our method is the idealized river equations [43, 48]

$$\begin{aligned} \partial_t h + \partial_x(hu) = 0, \\ \partial_t(hu) + \partial_x(hu^2 + \tfrac{1}{2}gh^2) = sgh - \frac{r}{4}|u|u, \end{aligned} \tag{4.15}$$

which is a shallow water model describing the depth h and mean velocity u of a river. Here $g > 0$ is the magnitude of gravitational acceleration, s is the slope of the river bottom, and r is a phenomenological drag coefficient. System (4.13) is genuinely nonlinear and strictly hyperbolic with characteristic velocities

$$\Lambda_{\pm} = u \pm \sqrt{gh}. \tag{4.16}$$

The local relaxation approximation is identified with the behavior of solutions of (4.15) over long space and time scales such as those associated with the description of flooding. The parabolic behavior is governed by [7]

$$\partial_t h + \partial_x\left(\sqrt{4sg/r}\, h^{3/2}\right) - \partial_x\left[\sqrt{sg/r}\left(\frac{1}{s} - \frac{1}{r}\right) h^{3/2}\partial_x h\right] = 0, \tag{4.17a}$$

$$u = \sqrt{4sg/r}\, h^{1/2} - \sqrt{sg/r}\left(\frac{1}{s} - \frac{1}{r}\right) h^{1/2}\partial_x h, \tag{4.17b}$$

provided the slope and drag satisfy $r > s$, which is just the stability condition (4.6).

The modified numerical flux for system (4.17) is given by

$$\begin{aligned} (HU)_{j+1/2} &= a_{j+1/2} H^{(1)}_{j+1/2} U^{(1)}_{j+1/2} + (1 - a_{j+1/2})\sqrt{4sg/r}\, H^{(2)^{3/2}}_{j+1/2} \\ &\quad - \sqrt{sg/r}\left(\frac{1}{s} - \frac{1}{r}\right)\frac{1 - a_{j+1/2}}{\Delta x} H^{(2)^{3/2}}_{j+1/2}(H_{j+1} - H_j), \end{aligned} \tag{4.18}$$

where $H^{(1)}_{j+1/2}$ and $U^{(1)}_{j+1/2}$ are given by a higher order Godunov scheme using the solution of the Riemann problem of the shallow water equations

$$\begin{aligned} \partial_t h + \partial_x(hu) = 0, \\ \partial_t(hu) + \partial_x(hu^2 + \tfrac{1}{2}gh^2) = 0, \end{aligned} \tag{4.19}$$

where $H^{(2)}_{j+1/2}$ is given by the same Godunov scheme for the solution of Riemann problem of the scalar conservation law

$$\partial_t h + \partial_x\left(\sqrt{4sg/r}\, h^{3/2}\right) = 0. \tag{4.20}$$

In this system the relaxation time and the characteristic variable are given by

$$\tau(h) = \sqrt{h/rsg}, \quad c(h) = \left(\frac{4s}{r} + 1\right)\sqrt{gh},$$

which follows from the general definition given in (4.7). The weight factor a is defined in a similar manner as in (4.13).

Remark. One can also define c as the maximal eigenvalue. However, our numerical experiments showed little differences between these two choices.

We first test these schemes in regimes where the long-time behavior becomes important. We choose the initial conditions

$$h(0, x) = 1 + 0.95 \sin(\pi x), \quad w(0, x) = 0, \qquad (4.21)$$

for $x \in [0, 1]$ with periodic boundary conditions and $r = 1000$, $s = 5$, $g = 1$. For this problem c ranges between 1.1414 and 1.6142. We compare these schemes by choosing $\Delta x = 0.1$, which gives a Pe ranging between 3.0975 and 6.1950. The results at $t = 1$ are depicted in Fig. 4. The "exact" solution is computed with PPM by taking $\Delta x = 0.001$. One can see that vL and PPM decay very rapidly while MvL and MPPM decay at speeds a lot closer to the physical one.

Finally we test the schemes for a problem in its strongly nonlinear regime with a thin viscous shock layer. Using this problem we test the performance of the modified schemes in the intermediate regimes. We choose $r = 400$, $s = 100$, and $g = 1$. The initial condition is chosen to be

$$h(0, x) = \begin{cases} 1 & \text{for } 0 < x < 0.5, \\ 0.2 & \text{for } 0.5 < x < 1, \end{cases} \quad w(0, x) = 0. \qquad (4.22)$$

We apply reflecting boundary conditions. In this problem there is a thin viscous shock layer moving to the right. If $\mathrm{Pe} \gg 1$ then all schemes give underresolved, non-oscillatory shock profile within two to three spatial cells. The physical viscous layer cannot be resolved in the coarse regime. To see the behavior of these schemes in the intermediate regime, we use 200 points on [0, 1]. Then Pe ranges between 0.5 and 2.5. The results at $t = 0.25$ are depicted in Fig. 5. The "exact" solution was obtained with PPM for $\Delta x = 10^{-3}$. It can be seen that all four schemes give comparable results which correctly resolve the physical viscous layer. Thus the modified schemes also give satisfactory results (comparable to the unmodified ones) in the intermediate regimes.

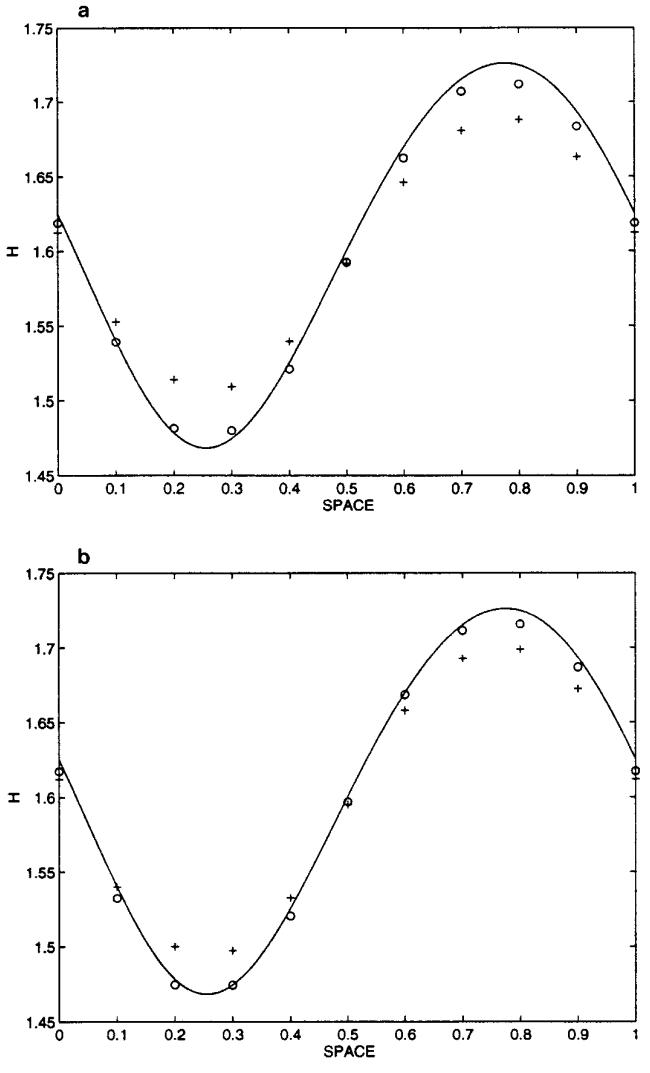

FIG. 4. Numerical vs exact solution of the river equations (4.14) and (4.21) at $t = 1$. Our "exact" solution (the solid lines) is obtained by PPM with $\Delta x = 0.001$. Numerical solutions are obtained with $\Delta x = 0.1$. In this example Pe ranges between 3.0975 and 6.1950. Upper: vL (+) and MvL (o) vs exact. Below: PPM (+) and MPPM (o) vs exact.

5. CONCLUSIONS

We have introduced a modification of Godunov schemes that gives the correct long-time behavior for hyperbolic systems with stiff relaxation terms. These methods are based on the asymptotic analysis of the long-time behavior of the solution that shows a balance between the relaxation terms and spatial derivative terms. Although we carry out our analysis and numerical experiments on simple 2×2 systems here, the spirit of the analysis extends to more complicated systems such as those mentioned in the beginning of the introduction. In particular, these ideas may be helpful in numerically understanding kinetic equations close to their macroscopic limit described by either the Euler or Navier–Stokes equations [2–4, 33].

We have only examined semidiscrete schemes in this article; the time steps in our numerical experiments being small enough so that no new errors were introduced to

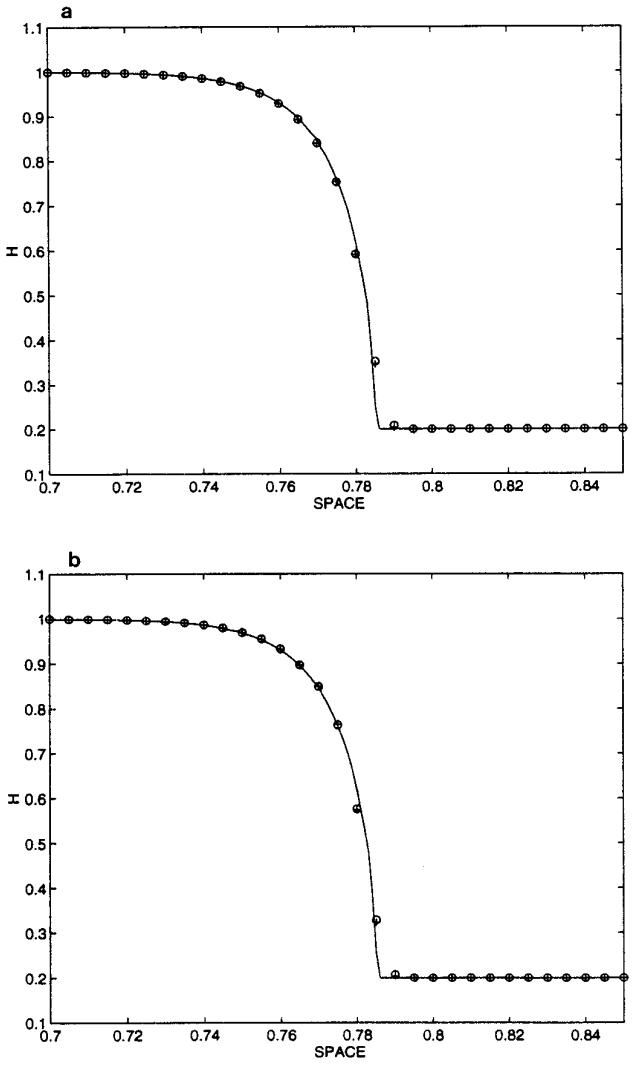

FIG. 5. Numerical vs exact solution of the river equations (4.14) and (4.22) at $t = 0.25$. Our "exact" solution (the solid lines) is obtained by PPM with $\Delta x = 0.0005$. Numerical solutions are obtained with $\Delta x = 0.005$. In this example Pe ranges between 0.5 and 2.5. Upper: vL (+) and MvL (o) vs exact. Below: PPM (+) and MPPM (o) vs exact.

affect our asymptotic analysis. However, in most applications one would not want to be limited to resolving such small time steps. The question about the possibility of using a coarse temporal discretization (a time step not limited by ε) naturally arises. Similar asymptotic analysis to that used here can be applied to study such fully discrete numerical schemes and is the subject of a forthcoming paper [24].

ACKNOWLEDGMENTS

S.J. is grateful to the University of Arizona and the Institute for Advanced Study for their support and to the support from AFOSR under Grant F49620-92-J0098 and NSF under Grant DMS-9404157. C.D.L. is grateful to the NSF for support under Grant DMS-8914420 and the AFOSR for support under Grant F49620-92-J0052. Both authors are grateful to the Arizona Center for Mathematical Sciences (ACMS) for its partial support. The ACMS is sponsored by the AFOSR under Contract AFOSR-90-0021 with the University Research Initiative Program at the University of Arizona. In addition, S.J. thanks J. M. Hyman, R. Indik, and M. Brio for many helpful discussions. We also thank the referees for their valuable comments.

REFERENCES

1. M. Ben-Artzi, *J. Comput. Phys.* **81,** 70 (1989).
2. R. Caflisch, *Commun. Pure Appl. Math.* **22,** 521 (1979).
3. R. Caflisch, S. Jin, and G. Russo, *SIAM J. Numer. Anal.,* to appear.
4. R. Caflisch and G. Papanicolaou, *Commun. Pure Appl. Math.* **32,** 589 (1979).
5. C. Cercignani, *The Boltzmann Equation and Its Applications* (Springer-Verlag, New York, 1988).
6. G.-Q. Chen and T.-P. Liu *Commun. Pure Appl. Math.* **45,** 755 (1993).
7. G.-Q. Chen, C. D. Levermore, and T.-P. Liu, *Commun. Pure Appl. Math.* **47,** 787 (1994).
8. J. F. Clark, *Rep. Prog. Phys.* **41,** 807 (1978).
9. P. Colella, A. Majda, and V. Roytburd, *SIAM J. Sci. Statist. Comput.* **7,** 1059 (1986).
10. P. Collela and P. R. Woodward, *J. Comput. Phys.* **54,** 174 (1984).
11. B. Engquist and B. Sjogreen, "Numerical Approximation of Hyperbolic Conservation Laws with Stiff Source Terms," in *Proceedings, Third International Conf. on Hyperbolic Problems,* edited by B. Engquist and B. Gustafsson (Studentlitteratur, 1991), p. 848.
12. B. Engquist and B. Sjogreen, UCLA CAM Report 91-03 (unpublished).
13. M. M. Gibson and B. E. Launder, *J. Fluid Mech.* **86,** 491 (1978).
14. H. M. Glaz and T.-P. Liu, *Adv. Appl. Math.* **29,** 1244 (1992).
15. J. Glimm, "The Continuous Structure of Discontinuities," Lecture Notes in Physics, Vol. 344 (Springer-Verlag, New York/Berlin, 1986), p. 177.
16. S. K. Godunov, *Mat. Sb.* **47,** 271 (1959).
17. F. Golse, S. Jin, and C. D. Levermore, *SIAM J. Numer. Anal.,* submitted.
18. D. F. Griffiths, A. M. Stuart, and H. C. Yee, *SIAM J. Numer. Anal.* **29**(5), 1244 (1992).
19. E. Harabetian, *SIAM J. Numer. Anal.* **27,** 870 (1990).
20. E. Harabetian, *J. Comput. Phys.* **103,** 350 (1992).
21. A. Harten, B. Engquist, S. Osher, and S. R. Chakravarthy, *J. Comput. Phys.* **71,** 231 (1987).
22. L. Hsiao and T.-P. Liu, *Commun. Math. Phys.* **143,** 599 (1992).
23. S. Jin, Ph.D. thesis, University of Arizona, 1991.
24. S. Jin, *J. Comput. Phys.* **122,** 51 (1995).
25. S. Jin and D. Levermore, *Transp. Theory Stat. Phys.* **20,** 413 (1991).
26. S. Jin and C. D. Levermore, *Transp. Theory Stat. Phys.* **22,** 739 (1993).
27. D. D. Joseph, *Fluid Dynamics of Viscoelastic Liquids* (Springer-Verlag, New York, 1990).
28. E. W. Larsen, *Nucl. Sci. Eng.* **112,** 336 (1992).
29. E. W. Larsen, J. E. Morel, and W. F. Miller Jr., *J. Comput. Phys.* **69** 283 (1987).
30. B. E. Launder and N. Shima, *AIAA J.* **27,** 1319 (1989).
31. R. J. LeVeque, *Numerical Methods for Conservation Laws* (Birkhäuser, Basel, 1992).
32. R. J. LeVeque and H. C. Yee, *J. Comput. Phys.* **86,** 187 (1990).
33. C. D. Levermore, "Fluid Dynamical Limits of the Discrete Kinetic

Theories,'' in *Macroscopic Simulations of Complex Hydrodynamic Phenomena,* edited by M. Mareschal and B. L. Holian, NATO ASI Series B, Vol. 292 (Plenum Press, New York, 1992), p. 173.

34. C. D. Levermore, *J. Stat. Phys.,* to appear.
35. T.-P. Liu, *Commun. Math. Phys.* **68,** 141 (1979).
36. T.-P. Liu, *Commun. Math. Phys.* **108,** 153 (1987).
37. H. Nessyahu and E. Tadmor, *J. Comput. Phys.* **87,** 408 (1990).
38. R. Pember, *SIAM J. Appl. Math.* **86,** 1293 (1993).
39. R. Pember, *SIAM J. Sci. Stat. Comput.* **14,** 824 (1993).
40. P. L. Roe, ''Upwind Differencing Schemes for Hyperbolic Conservation Laws with Source Terms,'' Lect. Notes in Math, Vol. 1270 (Springer-Verlag, New York/Berlin, 1986), p. 41.
41. P. L. Roe and M. Arora, *Numer. Methods Partial Differential Equations* **9,** 459 (1993).
42. J. Smoller, *Shock Waves and Reaction-Diffusion Equation* (Springer-Verlag, New York, 1983).
43. J. J. Stoker, *Water Waves* (Interscience, New York, 1966).
44. B. van Leer, *J. Comput. Phys.* **32,** 101 (1979).
45. B. van Leer, *SIAM J. Sci. Stat. Comput.* **5,** 1 (1984).
46. W. Vicenti and C. Kruger, *Introduction to Physical Gas Dynamics* (Kreger, Malabar, India, 1982).
47. R. F. Warming and B. J. Hyett, *J. Comput. Phys.* **14,** 159 (1973).
48. G. B. Whitham, *Linear and Nonlinear Waves* (Wiley-Interscience, New York, 1974).